Journal of Civil Engineering and Construction 2021;10(3):123-139
https://doi.org/10.32732/jcec.2021.10.3.123

# Vibration Mitigation of Wind Turbine Towers Using Negative Stiffness Absorbers

Konstantinos A. Kapasakalis[1], Ioannis A. Antoniadis[2], Evangelos J. Sapountzakis[1], Andreas E. Kampitsis[1]

*1. Institute of Structural Analysis and Antiseismic Research, School of Civil Engineering, National Technical University of Athens, Zografou Campus, GR-157 80 Athens, Greece*
*2. Dynamics and Structures Laboratory, School of Mechanical Engineering, National Technical University of Athens, Zografou Campus, GR-157 80 Athens, Greece*
*E-mail: kostiskapasakalis@hotmail.com; antogian@central.ntua.gr; cvsapoun@central.ntua.gr; cvakamb@gmail.com*

Received: 24 March 2021; Accepted: 22 April 2021; Available online: 5 June 2021

**Abstract:** The application of dynamic vibration absorbers (DVA) to Wind Turbine (WT) towers has the potential to significantly improve the damping of the tower and the nacelle dynamic responses, increasing thus the reliability of WTs. The Tuned Mass Damper (TMD) is limited by the requirement of large masses, in association to its installation location. In this study, two alternative concepts are considered. First, the nacelle is released from the WT tower, using a low stiffness connection. This option is based on the seismic isolation concept. Additionally, a novel passive vibration absorption configuration is implemented, based on the KDamper concept. The KDamper is essentially an extension of the TMD, introducing negative stiffness (NS) elements. Instead of increasing the additional mass, the vibration absorption capability of the KDamper can be increased by increasing the value of the NS element. Therefore, the KDamper always indicates better isolation properties than a TMD with the same additional mass. For the nonlinear dynamic response of the WT a build-in house software is developed. The dynamic performance of the proposed vibration mitigation concepts is numerically examined. All methods present superior dynamic behaviour as compared to the uncontrolled structure, however only the KDamper-based designs significantly increase the effective damping of the WT tower, retaining the additional masses in reasonable ranges.
**Keywords:** Wind turbines; Vibration control; Negative stiffness; KDamper; Effective damping.

## 1. Introduction

As wind power continues its rapid growth worldwide, wind farms are likely to comprise a significant portion of the total production of wind energy, and may even become a sizable contributor to the total electricity production in some countries. The high-quality wind resource and the proximity to load centres make wind energy a compelling proposition. The installed Wind Turbines (WT) energy potential is currently estimated at 539GW, according to the WWEA [1]. An important part of the WT network is the offshore wind turbines (OWT). OWT are expected to increase significantly as European coasts and seas offer a large wind energy potential. The WWEA predicts that offshore wind farms of 150GW will operate in the EU by 2030, contributing 14% of the EU's total electricity consumption.

However, the above prediction is very ambitious. It is noted, that in 2018 the annual rate of WT installation reached the lowest rate (10.8%) since the start of their industrial growth. Moreover, in recent years, several failures have been recorded in existing WT. It is estimated that the structural failure (tower, foundation) of the installed WT amounts up to 10% [2], significantly reducing their contribution to the energy network. These failures stem mainly from: i) WT collapse due to earthquake excitations, that cause structural failures due to high dynamic stress loading exciding structural strength, and ii) WT collapse due to wind loading, because of its continuous and cyclic nature, that causes failure due to structural fatigue. In addition, the structural and foundation costs are excessively high, reaching up to 17% for land based (onshore) and fixed bottom offshore WT, while when considering floating offshore WT the cost rises up to 40% [3–5].

From the above comments, and according to the International Energy Agency [6], it emerges as top priority to enhance research to avoid WT structural failures. A way to extend the feasibility of Wind Turbine towers is by means of structural control. The application of a vibration control system in a WT will result in a structural system with enhanced dynamic behavior under vibrating loading. It is classified as passive, active, hybrid, or semi-active control. Several researchers have been studying the use of structural control to help suppress the wind-induced

vibrations experienced by WT towers [7–10]. The passive control methods are simple and reliable, as they do not require an external force, are easy to implement to reduce the structural vibration, and are widely used in WT technology for enhancing their effective damping. The purpose of the installation of such devises, for the control of WT, is to mitigate their dynamic responses, due to the fact that the vibrations caused by aerodynamic loads are lasting and cause fatigue problems to the body of the tower, and to their foundation.

The concept of a resonant damper, like a Tuned Mass Damper (TMD) is among the approaches that have received the most attention in the literature. The principal of the TMD system [11] is the degradation of the dynamic response of the system through energy transfer to a system of an additional mass, designed with optimum characteristics and adapted in a suitable position in the structure [12,13]. The TMD system consist of an additional small mass and a positive stiffness element in combination with an artificial damper. The parameters that concern the design of such devices, are determined with the resonance of the frequency of the device with the fundamental eigenfrequency of the initial system. As a result, a great portion of the vibration energy of the structure, due to a vibratory excitation, is consumed by the additional mass of the device and then dissipated through the damper.

The Active Tuned Mass Damper (ATMD) is a hybrid devise consisting of a passive TMD supplemented by an actuator parallel to the spring and damper. It is a well-known concept in structural control and has been proved to yield enhanced damping performance compared to the passive TMD [14,15]. Semi-active TMDs are examined thoroughly recently, that introduce negative stiffness elements and negative stiffness tension adjusting mechanisms [16–20]. The downside of such designs is that their performance is directly (or obliquely) depended by the accuracy of the actuators output, which over time can have an alternation in its performance by false estimation of the desirable function of the vibration absorption concept and eventually burden the structure.

In addition, various forms of Dynamic Vibration Absorbers (DVA) have been used, such as Tuned Liquid Column Dampers (TCLDs) and multiple TMDs. Some of the pioneering work concerning applications in WTs include the work by [21] in which the damping effect of a TLCD installed in an offshore WT has been investigated by assuming correlated wind and wave load conditions, whereas the potential of using a pair of TMDs simultaneously targeting the dominant fore-aft ad side-side modes has been demonstrated by [10]. More recently, attention has focused on how to address the absence of aerodynamic damping in the side-side direction, when significant wind-wave misalignment is present, e.g. in the work by [9] where the beneficial of a TMD in reducing the tower base moment is demonstrated through numerical simulation, and in particular, a significant reduction in the side-side moment has been reported.

The essential limitations of all the aforementioned TMD-related concepts, are related with the location and the selected mass of these devices. In order to be effective, a resonant damper like the TMD should be installed where the absolute motion of the targeted vibration mode is largest, which is at the top of the tower or inside the nacelle. Effective damping by a TMD is furthermore associated with large additional masses, which constitutes a major limitation, since additional mass is highly undesirable at the top of the WT. In addition, a slight alteration in the control system parameters can alter the TMD tuning and consequently the system's performance is significantly reduced [22].

In this paper, two alternative vibration absorption approaches for mitigation of the WT dynamic responses are considered. First, the nacelle is released from the WT tower (nacelle isolation concept), using a low stiffness connection. This option is based on the seismic isolation concept of structures. This way, the nacelle is no longer rigidly connected to the WT tower, but is connected with a low stiffness element (elastomeric bearings). In order to retain the relative displacements of the nacelle-WT tower, an energy dissipation mechanism is implemented to reduce and control the displacements. In the second option, the KDamper (or an extension of it) is intervened between the nacelle and the WT tower. The KDamper, introduced in [23], is essentially an extension of the classical TMD, by incorporating appropriate negative stiffness elements. Instead of increasing the additional mass, the vibration isolation capability of the KDamper can be increased by increasing the value of the negative stiffness element, overcoming the sensitivity problems of TMDs as the tuning is mainly controlled by the negative stiffness element's parameters. Thus, the KDamper always indicates better isolation properties than a TMD with the same additional mass, finding numerous applications for vibration absorption of structural systems [24–30]. Although the KDamper incorporates a negative stiffness element, it is designed to be both statically and dynamically stable.

This paper is structured as follows. In Section 2 the vibration control approaches under consideration are presented, along with the dynamic model of the WT tower. The developed model is an assemblage of prismatic beam elements with sway degrees of freedom considered to be the dynamic degrees of freedom. In order to verify the validity and the efficiency of the developed formulation, a set of simplified analyses were conducted and the obtained results were compared with those obtained from the commercial software package SOFiSTiK (FEM Software for Structural Engineers | SOFiSTiK AG, n.d.) based on FEM. The aerodynamic load is taken into account by generating artificial basic wind velocities following the corresponding regulations of EC1, Part1,4 (EN 1991 - Wind actions, 2010) and applying it at the WT following the procedure described in [33]. Section 3, presents the optimization procedure from which the optimal parameters of the KDamper, and the extended versions of it, are obtained. The free design variables are presented, and proper limitations and constraints are imposed on the

free design variables and the system main dynamic responses, respectively, based on the proposed engineering-criteria driven optimization procedure. The NS element is realistically designed with a displacement-dependent configuration using pre-compressed positive stiffness elements (spiral springs), that generates 'linear' two-dimensional negative stiffness. Furthermore, the optimum design approach for the selection of the controlled WT with a TMD and the nacelle-isolation concept is presented. In section 4, a numerical example is presented, where the effectiveness of the proposed KDamper-based vibration mitigation approaches is verified. Based on a comparison with a conventional TMD (5% additional mass), and the proposed nacelle-isolation concept, the KDamper designs (0.1% additional mass) manage to significantly increase the effective damping of the WT tower, and thus mitigate the WT dynamic responses, with small additional masses and a realistically designed configuration. In section 5, the conclusive remarks are presented, and finally, in Appendix A, the formation of the submatrices of the controlled WT tower is presented considering all the vibration control approaches.

## 2. Methodology and modeling

This section presents the vibration mitigation approaches considered in this paper. The developed dynamic model of the wind turbine tower is an assemblage of prismatic beam elements with sway degrees of freedom considered to be the dynamic degrees of freedom. The validity and the efficiency of the developed formulation is verified with simplifies analyses, based on a comparison with a commercial software package, based on FEM [31]. Finally, the aerodynamic load is taken into account based on artificial wind basic velocities.

### 2.1 Vibration control approaches

Figure 1 presents the dynamic vibration absorber design options considered in this paper. The first vibration mitigation approach is the classical Tuned Mass Damped (TMD). The schematic representation of the TMD concept implemented in WT is depicted in the same figure, where the additional mass ($m_D$) of the TMD is attached at the top of the WT tower or inside the nacelle, using a positive stiffness element and a linear damper ($k_D$, $c_D$). This concept is employed as a benchmark because it has received the most attention in the literature due to the simplicity of its implementation. The main drawback of this option is the need for large additional masses, in order for the TMD to achieve significant effective damping, as will be observed in the numerical results.

The second vibration absorption option is based on the TMD concept combined with the seismic isolation principle, where the superstructure is isolated from its base/foundation with a low stiffness connection. Figure 1 presents the schematic representation of the proposed vibration absorption concept, where the mass that corresponds to the mechanical parts (nacelle, rotor and blades) is used as the additional mass of a TMD. Thus, the additional mass concentrated mass at the top of the tower is no longer connected rigidly to the steel tower, but is realized with a stiffness connection and a linear damper ($k_D$, $c_D$), as in the case of the classical TMD concept. This system will be referred to hereafter as nacelle-isolation concept. The main drawback that is to be expected, is that in order to isolate the steel tower from the vibrations of the nacelle, large relative displacements between the nacelle and the steel tower are required, which may prohibit the good function of the wind turbine.

In an effort to combine the aforementioned vibration control options, exploiting their advantages without their respective drawbacks, the KDamper is employed. As in the case of the nacelle isolation concept, the additional mass of the nacelle, rotor and blades is no longer rigidly attached to the WT tower but is mounted on a KDamper device. In this concept, the additional oscillating mass of the KDamper ($m_D$) is connected with the nacelle with a positive stiffness element and a linear damper ($k_{PS}$, $c_{PS}$), and with the steel tower with a negative stiffness (NS) element ($k_{NS}$), and the steel tower is connected with the nacelle with a positive stiffness connection ($k_R$). This way, the KDamper aims to isolate the vibrations of the nacelle form the steel tower, as in the case of the nacelle-isolation concept, retaining the relative displacements nacelle-tower within reasonable ranges. In addition, the KDamper aims to increase the effective damping of the WT tower compared to the TMD with the same additional mass, as it has been proven that the KDamper always presents an improved dynamic behavior as compared to the TMD. Finally, two extended version of the KDamper are also presented in Figure 1. In the proposed extensions, the additional mass, $m_D$ is connected with the nacelle with a NS element and an artificial damper ($k_{NS}$, $c_{NS}$), and with the steel tower with a positive stiffness element ($k_{PS}$). The extended version of KDamper will be referred to hereafter as EKD. Finally, the EKD is equipped with an inerter (EKDI) that connects the top of the tower directly with the nacelle, and thus is parallel to the stiffness element $k_R$. The addition of the inerter aims to further reduce the vibrations of the WT tower retaining the relative displacement nacelle-WT tower within reasonable ranges.

### 2.2 Dynamic model of the wind turbine

In this section, the NREL baseline 5-MW nacelle and rotor, supported by a steel tower of 120 *m* height is examined. This choice is made due to the fact that is widely used in the literature as a benchmark option for vibration control of WT towers. The WT tower of variable tubular cross section supporting the NREL baseline 5-MW nacelle and rotor [34] is examined. The base diameter is 8.43*m* with steel thickness 4.8c*m*, the top diameter

is 3.87$m$ with thickness 2.5cm, the Young's modulus is taken as 210$GPa$, while the steel density is assumed 8.5$tn/m^3$ and damping ratio (all modes) of 1%. In order to take into account, the inertial forces applied by the mechanical parts (nacelle, rotor and blades), an additional concentrated mass $m_{top}$ = 403.22 $tn$ [34] is added at the top of the WT tower. The WT tower is modeled as an assemblage of beam elements with sway degrees of freedom considered to be the dynamic degrees of freedom. The theoretical development is based on the assumption that the cross-sectional dimension within the element remains the same, i.e. prismatic beam element. Additional assumptions made for the analytical formulation are: (i) the WT tower is considered to remain within the elastic limit under the aerodynamic loads, (ii) the effects of soil-structure-interaction (SSI) are not taken into consideration, and (iii) the axial DoFs are not considered in this formulation, as the purpose of this work is to mitigate the dynamic responses of the WT tower due to horizontal aerodynamic loads, and thus is reasonable to neglect them. Figure 1 presents the lumped mass model of the WT tower.

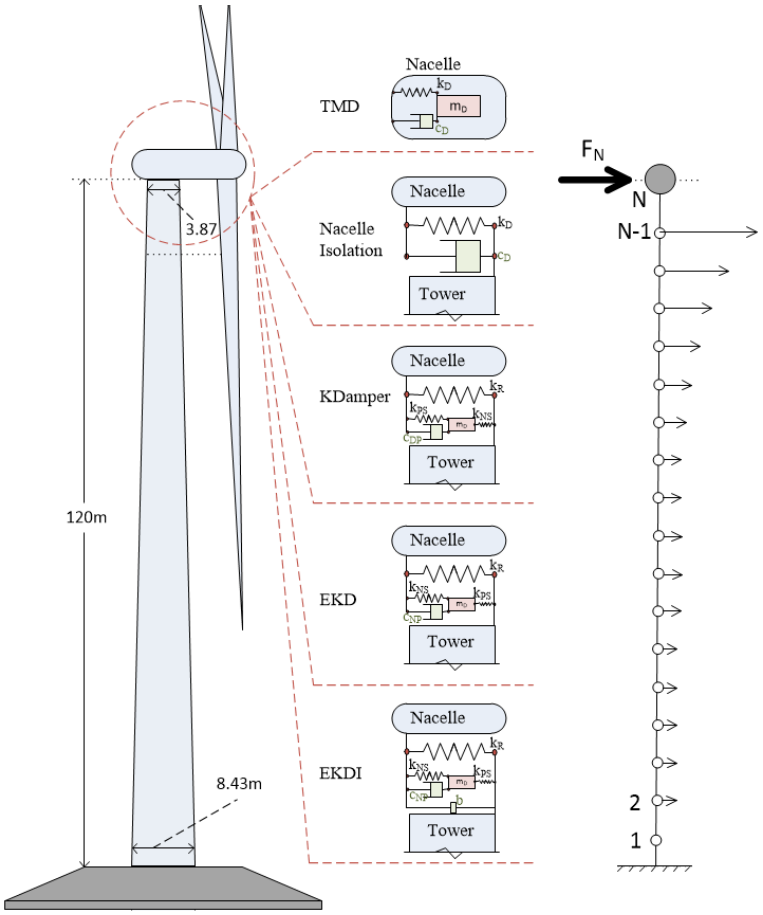


**Figure 1.** Vibration absorption concepts of the uncontrolled WT, TMD, nacelle-isolation, KDamper, EKD, and EKDI. The lumped mass model is used, with the sway as dynamic DoFs.

This model is serviceable due to the fact that it can incorporate easily each of the considered vibration absorption concepts, presented in section 2.1, and therefore evaluate their optimized parameters for vibration absorption, via optimization. The equations of motion of the uncontrolled WT, considering the equilibrium of forces at the location of each degree of freedom is expressed as follows:

$$[M_S]\{\ddot{u}_S\} + [C_S]\{\dot{u}_S\} + [K_S]\{u_S\} = [P_S] \quad (1)$$

where $[M_S]$, $[C_S]$ and $[K_S]$ are the mass, damping and stiffness matrices of the original WT tower, respectively of order ($N \times N$), $N$ indicating the number of prismatic beam elements selected to model the WT tower. The initial stiffness matrix is of order ($2N \times 2N$), as each beam element has two rotational and two sway DoFs, respectively. The condensed stiffness matrix of the uncontrolled WT tower is corresponding to the sway degrees of freedom, taken as the dynamic DoF, and thus is $[K_S]_{NxN}$. The damping matrix $[C_N]_{NxN}$ is not explicitly known but is obtained with the help of the Rayleigh's approach using the same damping ratio in all modes, 1% [34]. The unknown nodal displacements, relative to the base, are expressed as $ui$, and are collected in the array $\{u_S\} = \{u_1,u_2,u_3,\ldots,u_N\}^T$.

In order to verify the validity and the efficiency of the developed formulation, a set of simplified analyses were conducted and the obtained results were compared with those obtained from the commercial software package SOFiSTiK [31] based on FEM. More specifically, in Table 1, the first five eigenperiods of vibration, are presented using SOFiSTiK, and are compared with those obtained from a FEM solution employing 24 prismatic beam elements for the tower, the corresponding flexural modal shapes of the tower are illustrated. In Figure 2, the respective first five fundamental eigenshapes of the wind turbine are presented. It is observed that the largest amplitude at the top of the tower is presented at the first eigenshape followed by the second eigenshape. Thus, the tower response will be mainly determined by the first two vibration modes.

The response of the tower is examined performing a simplified linear static analysis, applying a concentrated force $\bar{F}_N = 1353.2kN$ (starting value of the generated aerodynamic load presented in section 2.3) at the top of the tower. Table 1 presents the static deflections $u_{top}$ at the top of the WT tower obtained from the developed model as compared with the aforementioned FEM solution, using SOFiSTiK software. It can be observed that the validity of the developed model of the WT tower is verified, as both the values of the WT eigenperiods and the static deflection of the top of the WT tower are in a very good agreement.

**Table 1.** Eigenperiods of the WT tower, and static deflection at the top of the tower under static analysis.

| | Natural Periods T (*sec*) | | | | | Static deflection at the top of the tower $u_{top}$ $(m)$ |
|---|---|---|---|---|---|---|
| | T1 | T2 | T3 | T4 | T5 | |
| Present study | 3.156 | 0.467 | 0.164 | 0.081 | 0.048 | 0.7063 |
| SOFiSTiK | 3.164 | 0.474 | 0.172 | 0.089 | 0.056 | 0.711 |

The governing equations of motion for the WT including the respective vibration mitigation concept to be considered are obtained by considering the equilibrium of forces at the location of each degree of freedom as follows:

$$[M]\{\ddot{u}\} + [C]\{\dot{u}\} + [K]\{u\} = [P] \tag{2}$$

where [*M*], [*C*] and [*K*] are the mass, damping and stiffness matrices of the controlled wind turbine tower, respectively of order (*N*+*n*) *x* (*N*+*n*). As stated previously, *N* indicates the wind turbine's DoFs and *n* the extra DoFs of each of the vibration isolation option to be considered. Furthermore, $\{u\} = \{\{u_N\}, \{u_n\}\}^T$ are the unknown, relative to the base, nodal displacements. The matrices of mass [*M*], damping [*C*], and stiffness [*K*] are of order (*N*+*n*) *x* (*N*+*n*), and are expressed as follows:

$$[M] = \begin{bmatrix} [M_S]_{N\times N} & [0]_{N\times n} \\ [0]_{n\times N} & [0]_{n\times n} \end{bmatrix} + \begin{bmatrix} [M_{n,a}]_{N\times N} & [0]_{N\times n} \\ [0]_{n\times N} & [M_{n,d}]_{n\times n} \end{bmatrix}_{(N+n)\times(N+n)} \tag{3.a}$$

$$[K] = \begin{bmatrix} [K_S]_{N\times N} & [0]_{N\times n} \\ [0]_{n\times N} & [0]_{n\times n} \end{bmatrix} + \begin{bmatrix} [K_{n,a}]_{N\times N} & -[K_{n,b}]_{N\times n} \\ -[K_{n,c}]_{n\times N} & [K_{n,d}]_{n\times n} \end{bmatrix}_{(N+n)\times(N+n)} \tag{3.b}$$

$$[C] = \begin{bmatrix} [C_S]_{N\times N} & [0]_{N\times n} \\ [0]_{n\times N} & [0]_{n\times n} \end{bmatrix} + \begin{bmatrix} [C_{n,a}]_{N\times N} & -[C_{n,b}]_{N\times n} \\ -[C_{n,c}]_{n\times N} & [C_{n,d}]_{n\times n} \end{bmatrix}_{(N+n)\times(N+n)} \tag{3.c}$$

where the submatrices [$M_{n,i}$], [$C_{n,i}$], and [$K_{n,i}$] (*i*=*a*, *b*, *c*, *d*) are expressed corresponding to the DoF associated with the respective control system to be considered. For the numerical modelling of the proposed formulation a build-in house software is developed in MATLAB code. The expressions of the additional matrices in Equations (3), that correspond to the employed vibration absorption concepts, are given in Appendix A.

## 2.3 Aerodynamic loads

The wind load varies along the height of the WT tower. The total horizontal wind force $\overline{F}_N(t)$ action on the blades can be calculated as three times the force $\hat{F}_N(r,t)$ acting at any position *r* along the single wind turbine blade. The $\hat{F}_N(r,t)$ accounts for the air density and the lift and drag coefficients as presented in [35]. The values of the latter coefficients depend on the airfoil characteristics of the blades and their distribution with respect to the angle of attack of the wind velocity $\overline{V}(t)$ passing through the blade profile. It is noted that $\overline{V}(t)$ is assumed to have a uniform spatial distribution over the actuator disc. In order to evaluate the horizontal wind force the blade element momentum theory incorporating Prandtl's tip loss factor and Glauert's correction [33] is employed with an

assumption of constant angular velocity of the blades. Subsequently, breaking $\overline{V}(t)$ down into a mean component $V_m$ and a fluctuating component $V$ $(t)$, the corresponding mean and fluctuating components of $\hat{F}_N(r,t)$ can be obtained as a mean force (steady state) and the dynamic part.

In this work, the mean velocity is obtained by employing a basic velocity at the altitude of $10m$, $V_b$ and applying the corresponding regulations of EC1, Part1,4 [32]. Moreover, in order to take into account, the wind velocity fluctuation at the altitude an artificial velocity time history is generated applying the procedures presented in [36–39] assuming a value of standard deviation $\sigma$. Apart from the concentrated force applied on the top of the steel tower due to operation of the turbine, an additional distributed loading along the tower height is taken into account due to the fact that a portion of wind forced is exerted directly on the tower. The spatial and time distribution of this loading is obtained by employing the procedures of (*EN 1991 - Wind actions*, 2010) and of the studies [36–38]. The basic wind velocity that is employed has corresponding standard deviation $V_b$=27.0$m/s$ with $\sigma$=3.3$m/s$ ($V_m$(120$m$)=39.93$m/s$). The rotor is assumed to develop a constant angular velocity 12.1$rpm$, while all the necessary blade profile characteristics are retrieved from [34,39]. Figure 3.a presents the wind velocity, and Figure 3.b the time history of the evaluated total forces.

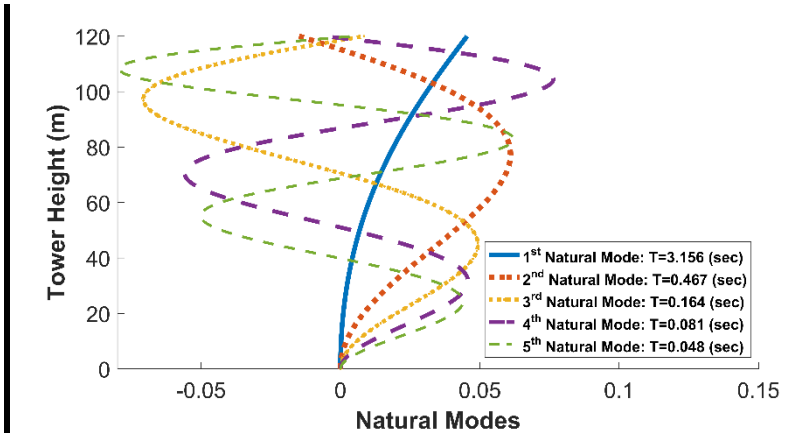


**Figure 2.** First five natural modes and eigenperiods of the uncontrolled WT.

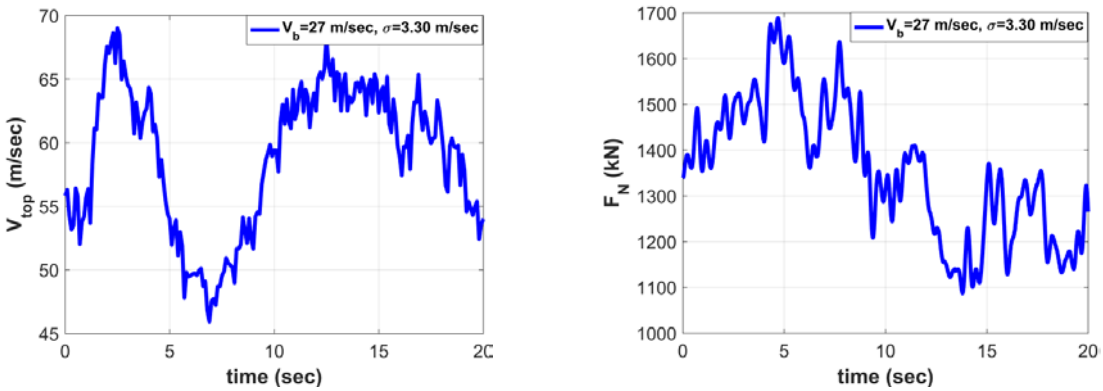


(a) (b)

**Figure 3.** Basic wind speed $V_b$ at the altitude of 10 m (a) and (b) time history of the total Force $\overline{F}_N(t)$ applied at the top of the wind turbine tower.

## 3. Optimal design of KDamper-based designs

In this section, an engineering-criteria driven optimization approach is followed for the selection of the proposed KDamper-based configuration parameters. The excitation input is generated according to section 2.3 of this paper. The free design variables of the devices implemented in between the nacelle and the WT tower are presented, and proper limitations and constraints are imposed on the free design variables and the system main dynamic responses, respectively. The NS element is realistically designed with a displacement-dependent configuration using pre-compressed positive stiffness elements, that generates 'linear' two-dimensional negative stiffness. The effectiveness of the proposed devices is evaluated by comparing its performance to a controlled system with a conventional TMD, and an alternative approach proposed in this paper, namely the nacelle-isolation concept presented in section 2.1 of this paper.

### 3.1 Free design variables

The Configurations of KDamper, extended KDamper (EKD), and EKD equipped with inerter (EKDI) are presented in section 2.1. The following positions concerning the KDamper concept, presented in Figure 1 are presented:

$$\mu_D = m_D/m_{top} \tag{4.a}$$

$$k_D = k_{NS} + k_{PS} \tag{4.b}$$

$$\omega_D = 2\pi f_D = \sqrt{k_D/m_D} = \sqrt{\frac{k_{NS}+k_{PS}}{m_D}} \tag{4.c}$$

$$k_0 = k_R + \frac{k_{NS}k_{PS}}{k_{NS}+k_{PS}} \tag{4.d}$$

$$\omega_0 = 2\pi f_0 = \sqrt{k_0/\left(m_D + m_{top}\right)} = \sqrt{\left(k_R + \frac{k_{NS}k_{PS}}{k_{NS}+k_{PS}}\right)/\left(m_D + m_{top}\right)} \tag{4.e}$$

$$\zeta_{PS} = c_{PS}/(2m_D\omega_D) = c_{PS}/(2\sqrt{k_D m_D}) \tag{4.f}$$

where $\mu_D$ is the mass ratio of the KDamper additional mass. The positions regarding the extended version of KDamper (EKD), and the EKD equipped with an inerter are exactly the same as with the KDamper. The EKDI is presented in Figure 1 where an inerter is implemented, connecting the nacelle directly with the WT tower. The inertance coefficient is expressed as follows:

$$\mu_b = m_b/m_{top} \tag{5}$$

where $\mu_b$ is the inertance mass ratio. In order for the proposed configuration to be realistic, the design of the KDamper-based designs foresees variation in all the stiffness elements to ensure that the system remain statically and dynamically stable:

$$(1-\varepsilon_R)k_R + \frac{(1-\varepsilon_{PS})k_{PS}(1+\varepsilon_{NS})k_{NS}}{(1-\varepsilon_{PS})k_{PS}+(1+\varepsilon_{NS})k_{NS}} = 0 \tag{6}$$

As a result, the stiffness elements $k_{PS}$ and $k_R$, result from Equations (4.e, 6) as a function of $f_0$, and $k_{NS}$. Therefore, assuming that the $m_D$, and the values of the stability factors $\varepsilon_{NS}$, $\varepsilon_{PS,}$ and $\varepsilon_R$ are supposed known, the free design variables sought in the optimization are:

1) the nominal frequency $f_0$;
2) the value of the negative stiffness (NS) element $k_{NS}$;
3) the value of the damping coefficient $c_{NS}$);
4) the value of the inerter $b$;

For the optimization process, the Harmony Search (HS) algorithm, a novel metaheuristic algorithm is used [40].

### 3.2 Realization of the negative stiffness element

Based on the proposed configuration for the realization of the negative stiffness element in [23] and [41], with pre-compressed springs, an alternative mechanism is hereby described, as depicted in Figure 4. The negative stiffness spring $k_N$ is realized by a linear vertical spring with constant $k_H$, which connects the additional mass $m_D$ and the structure by an articulated mechanism. Further information regarding the geometrical parameters of the proposed configuration presented in Figure 4.b, can be found in [23], the selection of which follows the procedure described also in [23]. The negative stiffness produced by the linear pre-compressed vertical spring, $k_H$, is given by:

$$k_{NS} = \frac{\partial f_N}{\partial u_{NS}} = -k_H\left[1 + c_I \frac{1}{(1-u_{NS}^2/a^2)^{3/2}}\right] \tag{7}$$

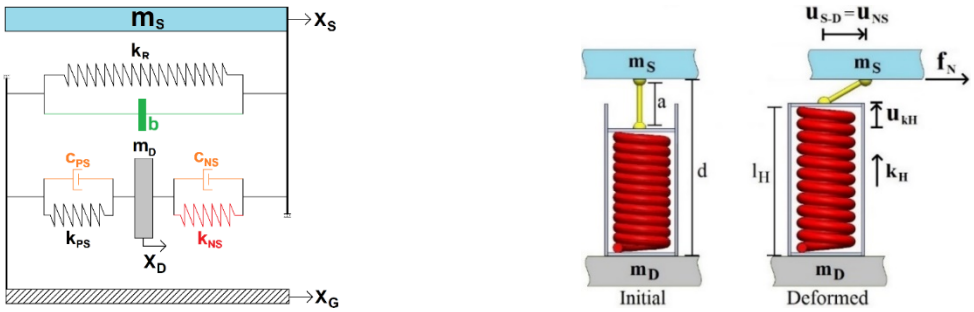


**Figure 4.** Schematic representation of the EKDI concept (a), and realization of the negative stiffness element (b).

### 3.3 Statement of the optimization problem

The purpose of the proposed vibration absorption configurations, based on the KDamper concept (KDamper, EKD and EKDI) is to enhance the dynamic performance of WT towers, by increasing the effective damping, and thus mitigate their dynamic responses. For the design to be realistic and efficient, at the same time, proper engineering criteria constraints and limitation must be applied in the system dynamic responses and free design variables, respectively. In particular:

1) The top displacement of the WT tower $u_{TOP}$ is set as the objective function.

2) A geometric limitation is imposed, regarding the relative displacement between the additional oscillating mass of the KDamper-based designs ($m_D$) and the top of the WT tower, $u_{D,REL}=u_D - u_{TOP}$. The upper limit of $u_{D,REL}$ is set equal to 1.5$m$, lower than half of the top diameter of the steel tower (3.84/2=1.92 $m$).

3) Another geometrical limitation is the nacelle's relative displacement with respect to the top of the wind turbine tower, $u_{NAC,\,REL}=u_{NAC} - u_{TOP}$. In order to ensure the effective operation of the WT, an upper limit of 0.5$m$ is placed in the $u_{NAC,\,REL}$.

4) The additional mass of the KDamper-based designs should be within reasonable ranges, since large masses constitute a major limitation, and are highly undesirable at the top of the wind turbine. For this reason, various sets of optimized EKDI parameters are selected for different values of the mass ratio $\mu_D$, in the range [0.1 0.5] %, more than one order of magnitude smaller as compared to the TMD concept.

5) The nominal frequency $f_0$ varies in the range *[0.1 2.0]* (*Hz*).

6) The upper limit of the inertance mass ratio $\mu_b$ is set equal to 0.5.

7) The damping coefficients maximum value $c_{PS}$ for the KDamper, and $c_{NS}$ for the extended KDamper designs, is set equal to *1000 kNs/m*, which based on previous work of KDamper is a realistic value for a superstructure mass 403.22 *tn*, which in this case is the concentrated mass at the top, $m_{top}$.

8) The NS element is realized with the proposed displacement-dependent configuration presented in section 3.2. The maximum (absolute) value is set equal to -50 *kN/m* per *tn* of structure mass, 50% lower as compared to the study of [23];

Finally, the limits of the free design variables are: a) the nominal frequency $f_0$ (*Hz*) [*0.1 2.0*], b) the negative stiffness element $k_{NS}$ (*kN/m*) [*-20000 -1*], c) the damping coefficient $c_{NS}$ and $c_{PS}$ (*kNs/m*) [*1 1000*], and the inertance mass ratio $\mu_b$ [0 0.5].

### 3.4 Comparison approaches

The considered comparison approaches selected to verify the effectiveness of the KDamper-based design concepts are the conventional TMD and the nacelle-isolation concept, presented thoroughly in section 2.1. The TMD system, consists of 3 elements, an additional mass, $m_D$, a positive stiffness element, $k_D$, and a linear damper, $c_D$. The following positions concerning the TMD design are introduced, considering implementation at the top of the WT tower or inside the nacelle, as presented in Figure 1.

$$\mu_D = m_D/m_{top} \tag{8.a}$$

$$\omega_D = 2\pi f_D = \sqrt{k_D/m_D} \tag{8.b}$$

$$\zeta_D = c_D/(2\omega_D m_D) = c_D/\left(2\sqrt{k_D m_D}\right) \tag{8.c}$$

where $\mu_D$ is the mass ratio of the TMD. The WT tower is a MDoF structural system, therefore the TMD design is not straightforward. The TMD tuning frequency is usually selected to be equal to the fundamental frequency, $f_1$, of the primary structure. In order to verify that this approach is indeed optimum for the implementation of the TMD to a WT tower, the maximum top displacement over the TMD tuning frequency is illustrated in Figure 5,

for various values of the TMD damping ratio, and the aerodynamic load presented previously.

The optimum value of the TMD frequency is indeed near the fundamental frequency of the uncontrolled WT, and more specifically in the range [0.9 1.3]$f_1$. The optimum value observed from Figure 5a of the $f_D$ is 1.25 $f_1$, and this value is adopted in this study for the optimum tuning of the TMD. It is observed that the damping ratio $\zeta_D$ of the TMD does not significantly affects $u_{TOP}$ of the controlled system. However, from Figure 5.b, it is clear that the TMD stroke is directly affected by the $\zeta_D$. The $\mu_D$ of TMD is selected for the considered analysis as 5%.

In order to optimally select the TMD damping ratio, $\zeta_D$, the $u_{TOP}$ and the TMD stroke are plotted in Figure 6, over $\zeta_D$, for various values of the TMD mass ratio $\mu_D$. In this case, as stated previously, the TMD tuning frequency is selected to be equal to 1.25 $f_1$, and is 0.396 *Hz*. It is observed that in the range of $\zeta_D$ [5 15] %, the maximum $u_{TOP}$ are minimized. However, for greater values of $\zeta_D$ over 15%, $u_{TOP}$ is not much affected. At the same time, from Figure 6.b it is observed that as $\zeta_D$ increased, the TMD stroke decreases, as expected. Therefore, $\zeta_D$ is selected equal to 30%, to mitigate the response of the WT tower, and at the same time retain the TMD stroke as small as possible. This value of $\zeta_D$=30% is usually high for a large mass of $\mu_D$=5%, but for the purpose of the comparison it can be adopted, as we are not interested in a realistic design, but a comparison basis.

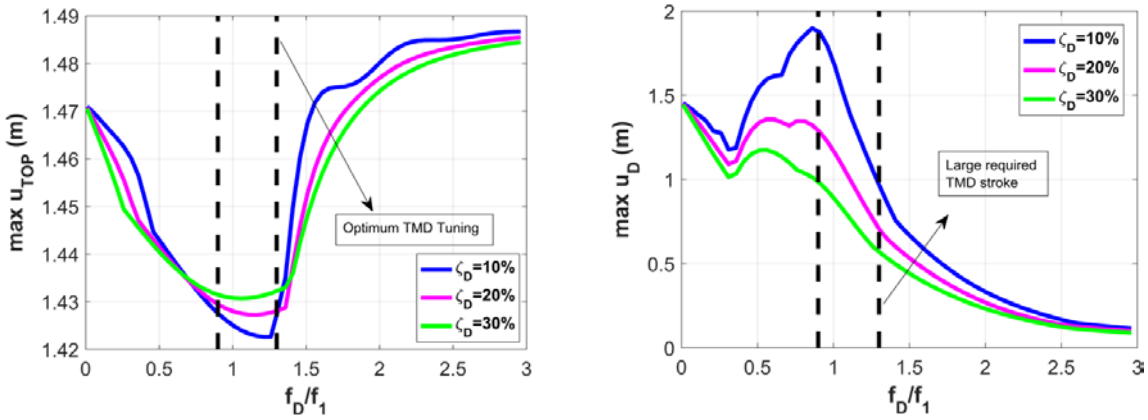


(a) (b)

**Figure 5.** Maximum top tower displacement (a), and TMD stroke (b) over nominal frequency ratio $f_D/f_1$, for various values of $\zeta_D$.

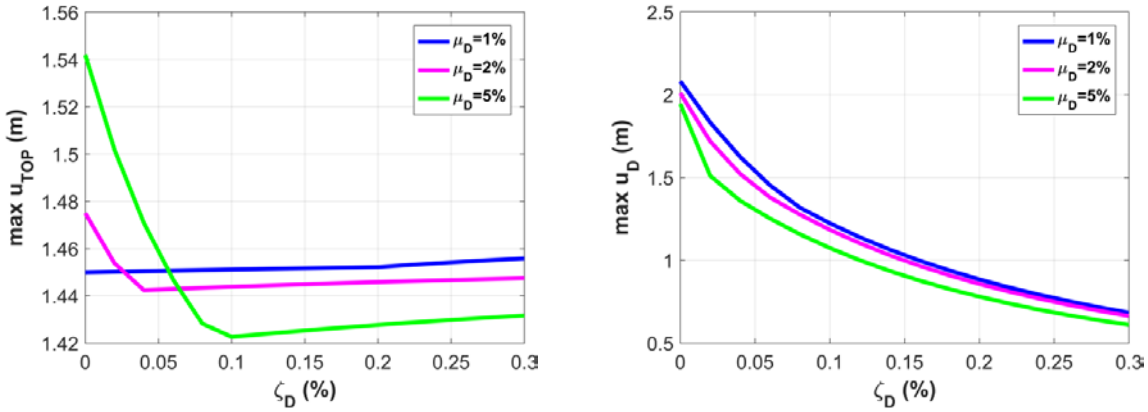


(a) (b)

**Figure 6.** Maximum top tower displacement (a) and TMD stroke(b) over $\zeta_D$, for various values of the $\mu_D$.

Figures 7.a, b present the effect of $\mu_D$, to the system main dynamic responses, i.e. $u_{TOP}$, and the TMD stroke. In addition, the effect of the implementation of the TMD to the $\zeta_{eff}$ of the WT tower is examined. In order to calculate the exact value of $\zeta_{eff}$, the system is subjected to a free vibration with initial conditions, according to the first modal eigenform of the uncontrolled WT. The initial condition of the TMD's DoF is selected to be equal to the one at the top of the WT. The $\zeta_{eff}$ is calculated according to the logarithmic rule, Equation (9) where T is the time between two consecutive peaks of $u_{TOP}$. Figure 7.c presents the effect of $\mu_D$ to the $\zeta_{eff}$.

$$\ln\left[\frac{u_{TOP}(t)}{u_{TOP}(t+T)}\right] = \frac{2\pi\zeta_{eff}}{\sqrt{1-\zeta_{eff}^2}} \tag{9}$$

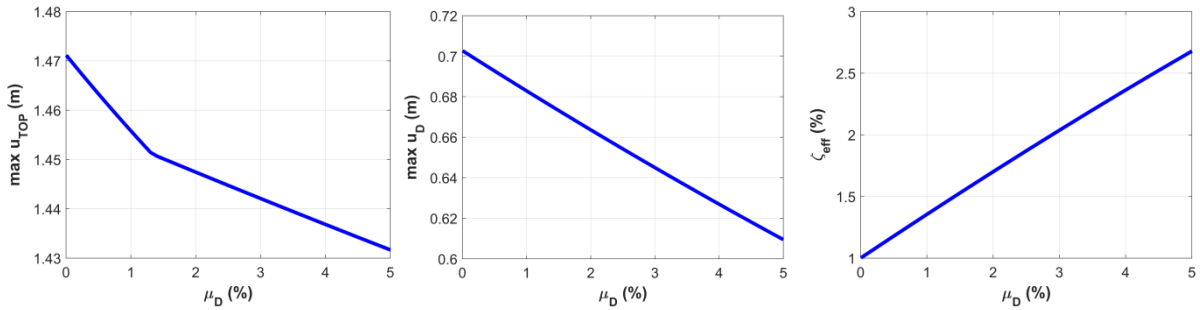


(a) (b) (c)

**Figure 7.** Effect of the TMD mass ratio $\mu_D$ to the top tower displacement(a), the TMD stroke (b), and the effective damping of the controlled system (c).

The increase of the additional mass ratio, $\mu_D$, greatly affects the top tower dynamic response, as expected. It is observed that as the $\mu_D$ increases the effect to the top displacement decreases. Furthermore, the mass ratio affects linearly the improvement of the TMD stroke, and the increase of the effective damping of the controlled system. Regarding the nacelle-isolation concept, the design parameters are the positive stiffness element $k_D$, and the artificial damper $c_D$. Based on the geometrical limitation presented for the KDamper-based designs, that the nacelle relative to the top of the tower displacement to be lower than 0.5 *m*, in order to have an equal comparison basis, the same constraint applies for the nacelle isolation concept. Furthermore, the maximum value of the $c_D$ is set to be equal to 1000 *kNs/m*, as in the KDamper-based designs. Parametric analyses are conducted and plotted in Figure 8, in order to select the optimum system parameters, reported in Equations (10).

$$\omega_D = 2\pi f_D = \sqrt{k_D/m_{tot}} \tag{10.a}$$

$$\zeta_D = c_D/(2\omega_D m_D) = c_D/\left(2\sqrt{k_D m_{tot}}\right) \tag{10.b}$$

In Figure 8.a, the nacelle, relative to the top tower, displacement, $u_{NAC,\,REL}$ is plotted over the tuning frequency $f_D$. It is observed that the tuning frequency of the nacelle-isolation concept is around 0.6 *Hz*, applying the constraint that the upper limit of the $u_{NAC,\,REL}$ is set to be equal to 0.5 *m*.

The damping ratio $\zeta_D$ does not affect the $u_{NAC,\,REL}$, as observed in Figure 8.a, but significantly affects $u_{TOP}$, which is the minimization goal of all the proposed vibration control strategies. For this reason, the damping ratio is selected to be equal to the upper limit ($c_{D,max}$=1000 *kNs/m*). The optimal system parameters of the nacelle-isolation concept therefore are $f_D$=0.556 *Hz* (limit case where $u_{NAC,\,REL}$=0.5 *m*), and $\zeta_D$=35.5 %.

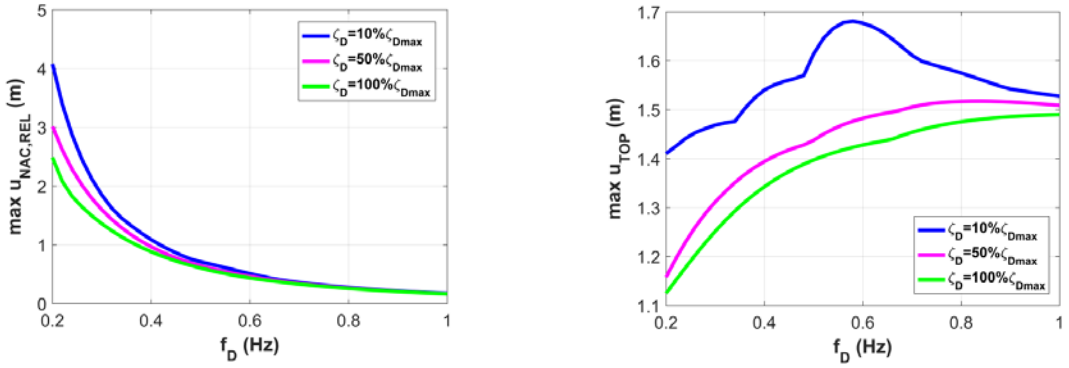


(a) (b)

**Figure 8.** Nacelle-isolation design. Tuning frequency (a) and damping ratio (b).

## 4. Numerical application – optimization results

In this section, the KDamper-based designs are implemented for vibration control in the considered WT. The optimal system parameters are selected following the optimization procedure described previously in section 3.3 of this paper. The parameters of the KDamper, EKD, and EKDI system are presented in Tables 2-4, respectively.

The WT tower dynamic responses and $\zeta_{eff}$ are illustrated in Figure 9, over the KDamper-based designs $\mu_D$, considering the optimized KDamper, EKD and EKDI vibration control configurations. In addition, the dynamic behavior of the nacelle is of great importance to the performance of the WT, and is greatly influenced by the

nacelle's angle of deflection, angular velocity, and relative (to the base) velocity. The aforementioned response variables of the nacelle, of the controlled system with KDamper, EKD, and EKDI are illustrated in Figure 10, over the $\mu_D$ of the respective system. Finally, the relative displacement of the additional mass, $m_D$, and the NS element stroke of all the KDamper-based designs are plotted in Figure 11, over the additional mass ratio, $\mu_D$.

**Table 2.** KDamper components.

| $\mu_D$ (%) | $f_0$ (Hz) | $k_{NS}$ (kN/m) | $c_{PS}$ (kNs/m) | $k_{PS}$ (kN/m) | $k_R$ (kN/m) |
|---|---|---|---|---|---|
| 0.1 | 0.547 | -3558.16 | 993.13 | 6714.58 | 12343.34 |
| 0.2 | 0.557 | -3492.81 | 966.73 | 6472.92 | 12538.02 |
| 0.3 | 0.547 | -3674.95 | 931.00 | 7006.28 | 12514.36 |
| 0.4 | 0.550 | -3371.66 | 831.60 | 6227.71 | 12181.48 |
| 0.5 | 0.548 | -3504.47 | 989.40 | 6564.08 | 12326.82 |

**Table 3.** Extended KDamper (EKD) components

| $\mu_D$ (%) | $f_0$ (Hz) | $k_{NS}$ (kN/m) | $c_{NS}$ (kNs/m) | $k_{PS}$ (kN/m) | $k_R$ (kN/m) |
|---|---|---|---|---|---|
| 0.1 | 0.541 | -9501.00 | 986.08 | 32385.78 | 18103.61 |
| 0.2 | 0.532 | -9335.64 | 968.12 | 32313.48 | 17638.61 |
| 0.3 | 0.532 | -8822.59 | 996.64 | 28789.43 | 17240.72 |
| 0.4 | 0.532 | -8758.40 | 963.99 | 28341.94 | 17201.80 |
| 0.5 | 0.523 | -8668.35 | 993.72 | 28732.58 | 16783.15 |

**Table 4.** Extended KDamper equipped with inerter (EKDI) components.

| $\mu_D$ (%) | $f_0$ (Hz) | $k_{NS}$ (kN/m) | $c_{NS}$ (kNs/m) | $\mu_b$ (%) | $k_{PS}$ (kN/m) | $k_R$ (kN/m) |
|---|---|---|---|---|---|---|
| 0.1 | 0.551 | -12543.61 | 997.34 | 0.498 | 58079.07 | 20829.40 |
| 0.2 | 0.545 | -10395.09 | 986.69 | 0.496 | 38285.04 | 19015.52 |
| 0.3 | 0.544 | -10380.34 | 960.28 | 0.497 | 38435.78 | 18938.34 |
| 0.4 | 0.538 | -8995.40 | 939.73 | 0.493 | 29242.48 | 17618.43 |
| 0.5 | 0.540 | -9086.47 | 996.11 | 0.497 | 29604.58 | 17772.91 |

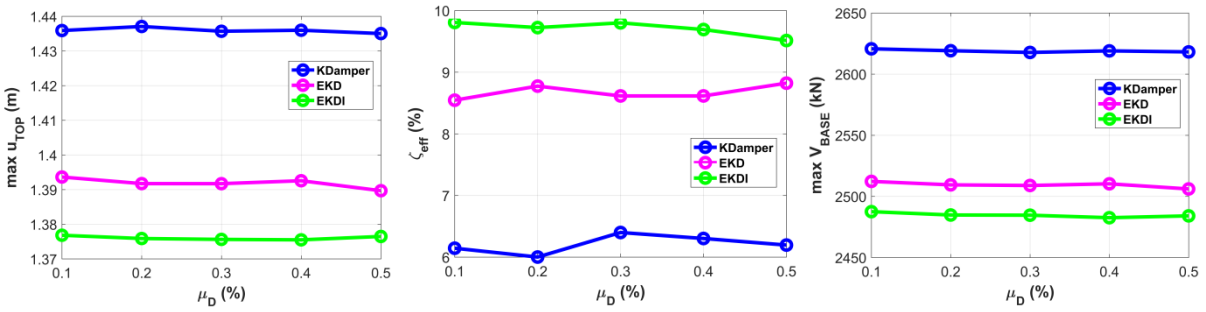


(a) (b) (c)

**Figure 9.** Optimization results for KDamper, EKD and EKDI. $u_{TOP}$ (a), $\zeta_{eff}$ (b), and $V_{BASE}$ (c).

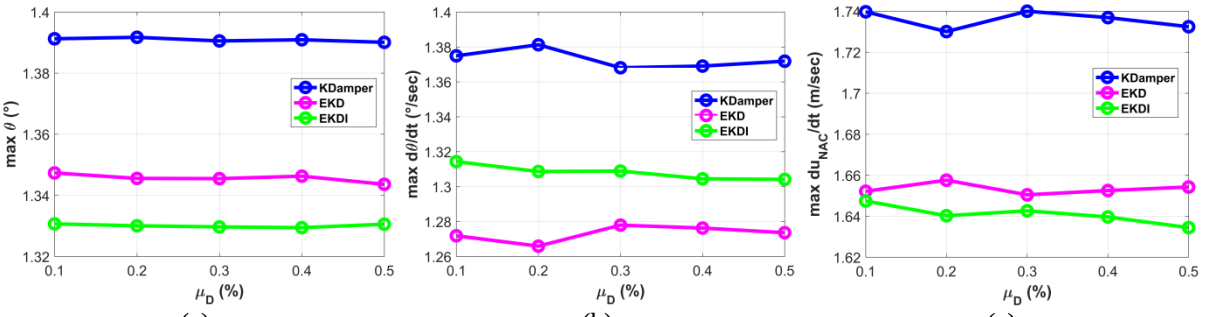


(a) (b) (c)

**Figure 10.** Optimization results for the KDamper, EKD and EKDI. Nacelle's angle of deflection (a), angular velocity (b), and relative (to the base) velocity (c).

In order to assess the effectiveness of the proposed absorbers, their performance is compared to a TMD and the nacelle-isolation concept, presented in section 2.1, and optimized for the specific implementation as presented in section 3. More specifically, the TMD has an $\mu_D$ of 5%, its nominal frequency is tuned to $1.25f_1$, and $\zeta_D$ is selected as 30%. The nacelle isolation concept is tuned to $f_D$=0.556 *Hz*, and the value of its $c_D$ is equal to 1000 *kNs/m*. The

maximum values of the dynamic responses and the $\zeta_{eff}$ of all the considered vibration control systems are collected in Table 5. Regarding the KDamper-based designs, the presented results concern the optimized sets of parameters with an $\mu_D$ of 0.1%. The KDamper-based designs manage to greatly improve the dynamic behavior of the WT tower. The $\zeta_{eff}$ of the WT tower increases up to 10% with the EKDI system. The nacelle's dynamic response variables are also improved, with the exception of the nacelle's relative velocity, where a slight increase is observed. In addition, EKD and EKDI, greatly reduce the $u_{NS}$ and $u_D$, making the configuration design more realistic. The dynamic responses of the WT tower and the nacelle's response variables, considering the TMD, the nacelle-isolation, and EKDI are illustrated in Figures 12, 13, respectively. Finally, the time history of the $u_{NS}$ and $u_D$ are illustrated in Figure 14 for all the KDamper-based designs.

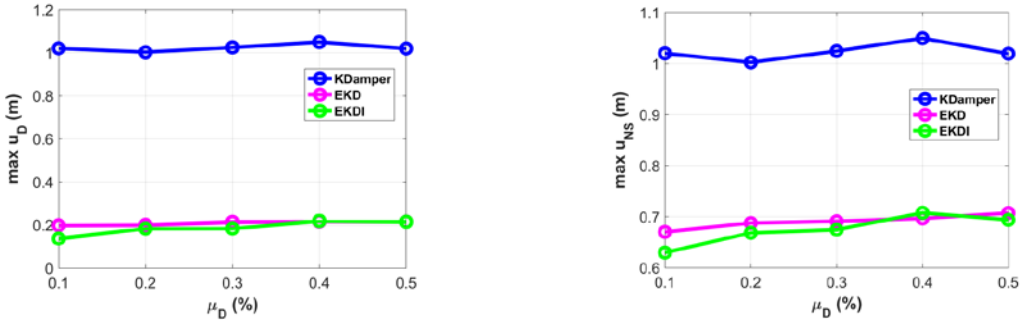


(a) (b)

**Figure 11.** Optimization results for the KDamper, EKD and EKDI. $u_D$ (a), and $u_{NS}$ (b).

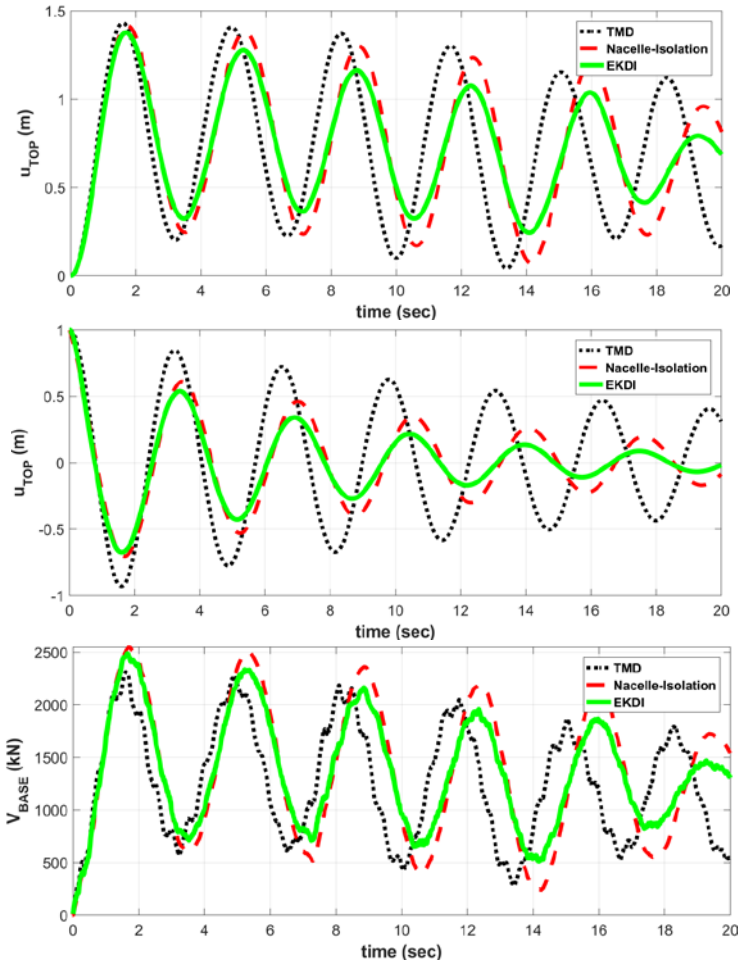


(a)

(b)

(c)

**Figure 12.** Dynamic responses of the controlled WT: top tower displacement due to the aerodynamic load (a), top tower displacement considering a free vibration with initial conditions (b), and base shear due to the aerodynamic load (c).

**Table 5.** Maximum values of the WT tower's effective damping ratio, $\zeta_{eff}$, dynamic responses of the WT tower and the respective control system, and the nacelle's response variables.

| | Dynamic Control system | | | | | |
|---|---|---|---|---|---|---|
| | Uncontrolled | TMD | Nacelle-isolation | KDamper | EKD | EKDI |
| $u_{TOP}$ $(m)$ | 1.471 | 1.429 | 1.4167 | 1.436 | 1.394 | 1.377 |
| $\zeta_{eff}$ $(\%)$ | 1 | 2.68 | 7.82 | 6.14 | 8.55 | 9.81 |
| $V_{BASE}$ $(kN)$ | 2677.6 | 2308.6 | 2547.1 | 2620.7 | 2512.3 | 2487.5 |
| $\theta$ $(^{\circ})$ | 1.424 | 1.391 | 1.368 | 1.391 | 1.347 | 1.331 |
| $d\theta/dt$ $(^{\circ}/sec)$ | 1.484 | 1.451 | 1.238 | 1.375 | 1.272 | 1.314 |
| $du_{NAC}/dt$ $(m/sec)$ | 1.448 | 1.406 | 1.703 | 1.740 | 1.652 | 1.647 |
| $u_D$ $(m)$ | - | 0.701 | 0.500 | 1.020 | 0.198 | 0.136 |
| $u_{NS}$ $(m)$ | - | - | - | 1.020 | 0.670 | 0.629 |

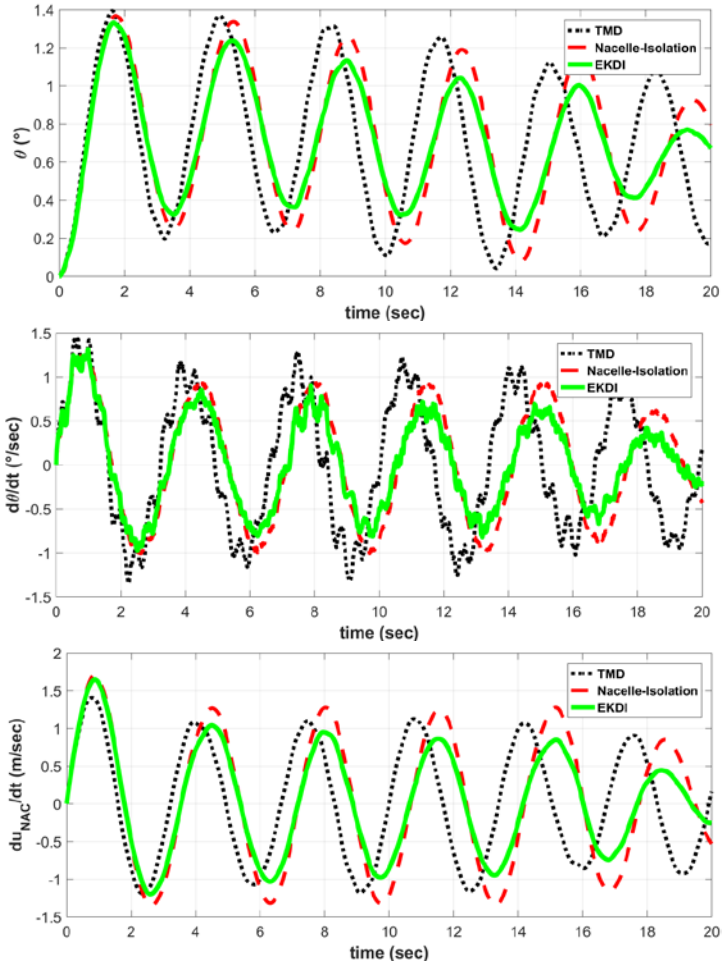


(a)

(b)

(c)

**Figure 13.** Nacelle's response variables of the controlled WT angle of deflection (a), angular velocity (b), and relative (to the base) velocity (c), due to the aerodynamic load.

## 5. Concluding remarks

In this paper, three dynamic vibration absorber options are examined for improving the WT tower dynamic behavior and increasing the effective damping, i.e. the conventional TMD, the nacelle-isolation concept, and three KDamper-based designs. A wind turbine of 5MW supported by a steel tower of 120 m was analyzed under a horizontal aerodynamic load due to the wind. The vibration mitigation approaches are presented, along with the dynamic model of the WT tower. The developed model is an assemblage of prismatic beam elements, the validity of which is verified based on a comparison with a commercial software package on FEM. The aerodynamic load is taken into account by generating artificial basic wind velocities applying the corresponding regulations of EC1, Part1,4. The TMD and the nacelle-isolation concepts, are optimally design for the specific implementation for the protection of the WT tower. An engineering-criteria optimization procedure is followed for the design of the

KDamper-based configurations. The NS element is realistically designed with a displacement-dependent configuration. Based on a comparison with a conventional TMD, and the proposed nacelle-isolation concept, the KDamper designs manage to significantly increase the effective damping, and thus mitigate the WT dynamic responses, with small additional masses and a realistically designed configuration. Finally, the following conclusive comments can be made:

1) The dynamic model of the WT tower developed here is serviceable due to the fact that it can incorporate easily each of the considered vibration absorption concepts, and the validity of the proposed formulation is verified as compared with a commercial software package based on FEM.

2) The increase of the effective damping of the WT tower is much greater with the implementation of the KDamper-based designs (6.14%, 8.55%, 9.81%), compared to that with a TMD (2.68%) with an additional mass of 5%, and the nacelle-isolation concept (7.82%).

3) The KDamper-based configurations are much more effective than the conventional TMD approach, employing a small additional mass of only 0.1%, 50 times lower compared to the TMD's.

4) Regarding the dynamic behavior of the WT tower, the KDamper-based concepts provided the best results followed by the TMD concept and the nacelle-isolation concept. More specifically, the tower's top displacement is reduced 2.38%, 5.23% and 6.39% with the KDamper-based concepts (0.1% mass ratio), 2.86% with the TMD concept (5% mass ratio) and 3.69% with the nacelle-isolation concept and the shear force of the tower is reduced 2.12%, 6.17% and 7.10% with the KDamper-based concepts, 13.78% with the TMD concept and 4.87% with the nacelle-isolation concept.

5) The use of a TMD has a small influence on the nacelle's response variables. The KDamper-based concepts, and the nacelle-isolation concept improve all the response variables of the nacelle, except for the maximum value of the nacelle's velocity which in the first peak of the dynamic response present a slight increase.

6) The proposed extensions of KDamper manage to significantly decrease the NS element stroke, making the device's design more realistic.

7) The addition of the inerter in the EKD configuration has a beneficial impact in the overall dynamic behavior of the WT.

According to the comments made above, the KDamper-based designs can provide a realistic alternative to the existing vibration absorption design options in WT towers, providing a great increase to the tower's damping as well as improving the dynamic performance both of the nacelle and the WT tower. The reliability and simplicity of the system are also advantages that render the device suitable for various technological implementations and competitive against other vibration absorption designs.

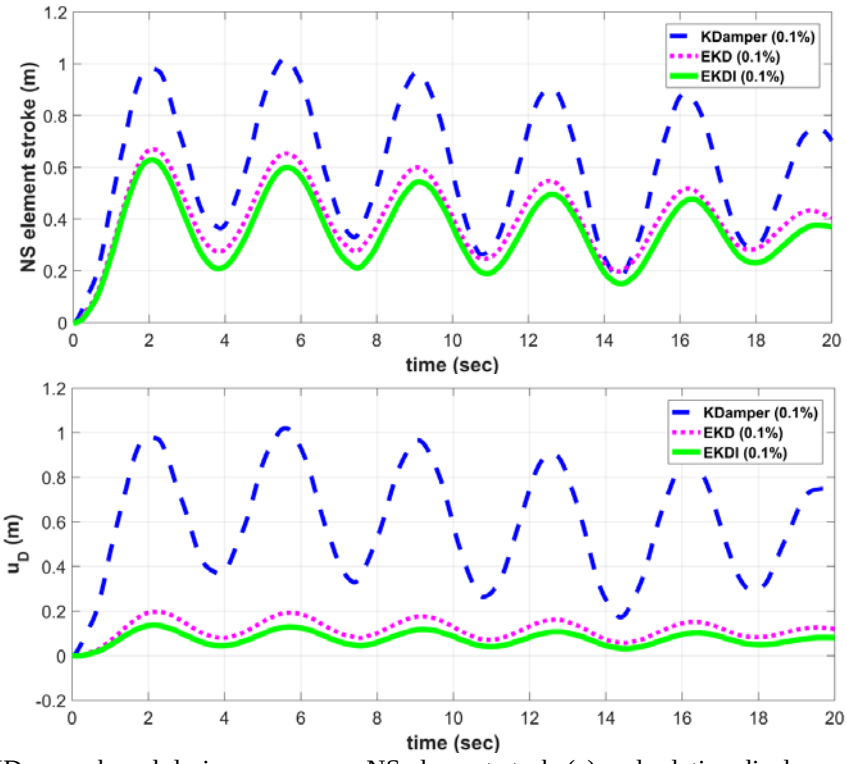


**Figure 14.** KDamper-based designs responses NS element stroke(a) and relative displacement of the oscillating mass with the top of the WT tower (b), due to the aerodynamic load.

## 6. Acknowledgments

This research has been co-financed by the European Union and Greek national funds through the Operational Program Competitiveness, Entrepreneurship and Innovation, under the call RESEARCH – CREATE – INNOVATE (project code: T1EDK-02827).

## 7. References

[1] Wind Power Capacity Reaches 546 GW, 60 GW Added in 2017 – World Wind Energy Association [Online]. Available from: https://wwindea.org/blog/2018/02/12/2017-statistics/. [Accessed: 22-Apr-2020].
[2] Li Y. Research and development of the wind turbine reliability. International Journal of Mechanical Engineering and Applications. 2018;6(2):35.
[3] Renewable Energy Agency. Renewable energy technologies: cost analysis series Volume 1: Power sector acknowledgement. 2012.
[4] Mone C, Hand M, Bolinger M, Rand J, Heimiller D, Ho J. 2015 Cost of Wind Energy Review. 2015.
[5] Morais M et al. Dynamic behavior analysis of wind turbine towers. 2009.
[6] Sustainable Development Scenario – World Energy Model – Analysis - IEA [Online]. Available from: https://www.iea.org/reports/world-energy-model/sustainable-development-scenario. [Accessed: 24-Apr-2020].
[7] Nigdeli SM, Bekdaş G..Optimum tuned mass damper design in frequency domain for structures. KSCE Journal of Civil Engineering. 2017;21(3):912–922.
[8] Avila S, Shzu M, Morais M, Prado Z. Numerical modeling of the dynamic behavior of a wind turbine tower. Advances in Vibration Engineering. 2016;4.
[9] Stewart G, Lackner M. The impact of passive tuned mass dampers and wind–wave misalignment on offshore wind turbine loads. Engineering Structures. 2014;73.
[10] Lackner MA, Rotea MA. Passive structural control of offshore wind turbines. Wind Energy. 2011;14(3):373–388.
[11] Frahm H. Device for damping of bodies. U.S. Pat., (989). 1911.
[12] Soong TT, Dargush GF. Passive energy dissipation systems in structural engineering. Wiley. 1997.
[13] Casciati F, Giuliano F. Performance of multi-TMD in the towers of suspension bridges. Journal of Vibration and Control. 2009;15(6):821–847.
[14] Ricciardelli F, Pizzimenti AD, Mattei M. Passive and active mass damper control of the response of tall buildings to wind gustiness. Engineering Structures. 2003;25(9):1199–1209.
[15] Ankireddi S, Yang HTY. Simple ATMD control methodology for tall buildings subject to wind loads. Journal of Structural Engineering 1996;122(1):83–91.
[16] Liao GJ, Gong XL, Kang CJ, Xuan SH. The design of an active–adaptive tuned vibration absorber based on magnetorheological elastomer and its vibration attenuation performance. Smart Matererials and Structures. 2011;20(7):075015.
[17] Weber F, Boston C, Maślanka M. An adaptive tuned mass damper based on the emulation of positive and negative stiffness with an MR damper. Smart Materials and Structures. 2011;20(1):015012.
[18] Casciati F, Rodellar J, Yildirim U. Active and semi-active control of structures – theory and applications: a review of recent advances. Journal of Intelligent Materials Systems and Structures. 2012;23(11):1181–1195.
[19] Acar MA, Yilmaz C. Design of an adaptive-passive dynamic vibration absorber composed of a string-mass system equipped with negative stiffness tension adjusting mechanism. Journal of Sound and Vibration. 2013;332(2):231–245.
[20] Weber F. Optimal semi-active vibration absorber for harmonic excitation based on controlled semi-active damper. Smart Materials and Structures. 2014;23(9):095033.
[21] Colwell S, Basu B. Tuned liquid column dampers in offshore wind turbines for structural control. Engineering Structures. 2009;31(2):358–368.
[22] Weber B, Feltrin G. Assessment of long-term behavior of tuned mass dampers by system identification. Engineering Structures. 2010;32(11):3670–3682.
[23] Antoniadis IA, Kanarachos SA, Gryllias K, Sapountzakis IE. KDamping: A stiffness based vibration absorption concept. Journal of Vibration and Control. 2018;24(3):588–606.
[24] Kapasakalis K, Sapountzakis E, Antoniadis I. Implementation of the KDamper concept to wind turbine towers. In: 6th International Conference on Computational Methods in Structural Dynamics and Earthquake Engineering (COMPDYN 2017). 2017.
[25] Kapasakalis K, Antoniadis I, Sapountzakis E. Control of multi storey building structures with a new passive vibration control system com-bining base Isolation with KDamper. In: 7th International Conference on Computational Methods in Structural Dynamics and Earthquake Engineering (COMPDYN 2019). 2019.

[26] Antoniadis I, Kapasakalis K, Sapountzakis E. Advanced negative stiffness absorbers for the seismic protection of structures. In: International Conference on Key Enabling Technologies 2019 (KEYTECH2019). 2019.
[27] Kapasakalis K, Antoniadis I, Sapountzakis E. Performance assessment of the KDamper as a seismic absorption base. structural control and health monitoring. https://onlinelibrary.wiley.com/doi/10.1002/stc.2482. 2019
[28] Kapasakalis K, Antoniadis I, Sapountzakis E. KDamper concept for base isolation and damping of high-rise building structures. In: 14th International Conference on Vibration Problems (ICOVP 2019). 2019.
[29] Kapasakalis K, Sapountzakis E, Antoniadis I. Optimal design of the KDamper concept for structures on compliant supports. In: 16th European Conference on Earthquake Engineering (16ECEE 2018). 2018.
[30] Kapasakalis KA, Antoniadis IA, Sapountzakis EJ. Constrained optimal design of seismic base absorbers based on an extended KDamper concept. Engineering Structures. https://www.sciencedirect.com/science/article/pii/S0141029620339134?via%3Dihub. 2021.
[31] FEM, BIM and CAD software for structural engineers | SOFiSTiK AG [Online]. Available from: https://www.sofistik.com/?__hstc=136929903.778d8a8e3515c0a0f7da049d7f27258a.1587748377743.1587748377743.1587748377743.1&__hssc=136929903.2.1587748377744&__hsfp=4014916924. [Accessed: 24-Apr-2020].
[32] EN 1991-1-4: Eurocode 1: Actions on structures - Part 1-4: General actions - Wind actions. 2010.
[33] Hansen ML. Aerodynamics of wind turbines, Earthscan. 2008.
[34] Quilligan A, O'Connor A, Pakrashi V. Fragility analysis of steel and concrete wind turbine towers. Engineering Structures. 2012;36:270–282.
[35] Sapountzakis EJ, Dikaros IC, Kampitsis AE, Koroneou AD. Nonlinear response of wind turbines under wind and seismic excitations with soil-structure interaction. Journa of Computational and Nonlinear Dynamics. 2015;10(4).
[36] Koulatsou K, Petrini F, Vernardos S, Gantes CJ. Artificial time histories of wind actionsfor structural analysis of wind turbines. 2013.
[37] Paola DM. Digital simulation of wind field velocity. Journal of Wind Engineering and Industrial Aerodynamics. 1998;(74–76):91–109.
[38] Norske Veritas (Organization), Forskningscenter Risø. Guidelines for design of wind turbines., Det Norske Veritas, Copenhagen ;[Roskilde Denmark]. 2002.
[39] Jonkman JM. Dynamics modeling and loads analysis of an offshore floating wind turbine. Technical Report No. NREL/TP-500-41958. 2007.
[40] Zong WG, Joong HK, Loganathan GV. A new heuristic optimization algorithm: Harmony search. Simulation. 2001;76(2):60–68.
[41] Carrella A, Brennan MJ, Waters TP. Static analysis of a passive vibration isolator with Quasi-Zero-Stiffness characteristic. Journal of Sound and Vibration. 2007;301(3–5):678–689.

## Appendix A: Formation of the DVA submatrices

### A.1 TMD

The controlled system has (*N*+1) dynamic DoFs, where *N* indicates the number of prismatic beam elements simulating the WT. The submatrices Equations (3) are expressed as follows:

$$[M_{n,a}] = [0]_{N\times N} \qquad [M_{n,b}] = [M_{n,c}]^T = \{0\}_{N\times 1} \qquad M_{n,d} = +m_D = +\mu_D m_{tot} \tag{A.1.1}$$

$$[K_{n,a}] = \begin{bmatrix} 0 & \cdots & 0 \\ \vdots & \ddots & \vdots \\ 0 & \cdots & +k_D \end{bmatrix}_{N\times N} \qquad [K_{n,b}]^T = [K_{n,c}] = [0 \quad \cdots \quad -k_D]_{1\times N} \qquad K_{n,d} = +k_D \tag{A.1.2}$$

$$[C_{n,a}] = \begin{bmatrix} 0 & \cdots & 0 \\ \vdots & \ddots & \vdots \\ 0 & \cdots & +c_D \end{bmatrix}_{N\times N} \qquad [C_{n,b}]^T = [C_{n,c}] = [0 \quad \cdots \quad -c_D]_{1\times N} \qquad C_{n,d} = +c_D \tag{A.1.3}$$

### A.2 Nacelle-isolation

The controlled system has (*N*+1) dynamic DoFs. The submatrices Equations (3) are expressed as follows:

$$[M_{n,a}] = \begin{bmatrix} 0 & \cdots & 0 \\ \vdots & \ddots & \vdots \\ 0 & \cdots & -m_{top} \end{bmatrix}_{N\times N} \qquad [M_{n,b}] = [M_{n,c}]^T = \{0\}_{N\times 1} \qquad M_{n,d} = +m_{top} \tag{A.2.1}$$

$$[K_{n,a}] = \begin{bmatrix} 0 & \cdots & 0 \\ \vdots & \ddots & \vdots \\ 0 & \cdots & +k_D \end{bmatrix}_{N\times N} \quad [K_{n,b}]^T = [K_{n,c}]_{1\times N} = [0 \quad \cdots \quad -k_D]_{1\times N} \quad K_{n,d} = +k_D \tag{A.2.2}$$

$$[C_{n,a}] = \begin{bmatrix} 0 & \cdots & 0 \\ \vdots & \ddots & \vdots \\ 0 & \cdots & +c_D \end{bmatrix}_{N\times N} \quad [C_{n,b}]^T = [C_{n,c}] = [0 \quad \cdots \quad -c_D]_{1\times N} \quad C_{n,d} = +c_D \tag{A.2.3}$$

**A.3 KDamper**

The controlled system has (*N*+2) dynamic DoFs. The submatrices Equations (3) are expressed as follows:

$$[M_{n,a}] = \begin{bmatrix} 0 & \cdots & 0 \\ \vdots & \ddots & \vdots \\ 0 & \cdots & -m_{top} \end{bmatrix}_{N\times N} \quad [M_{n,b}]^T = [M_{n,c}] = \{0\}_{2\times N} \quad [M_{n,d}] = \begin{bmatrix} +m_D & 0 \\ 0 & +m_{top} \end{bmatrix}_{2\times 2} \tag{A.3.1}$$

$$[K_{n,a}] = \begin{bmatrix} 0 & \cdots & 0 \\ \vdots & \ddots & \vdots \\ 0 & \cdots & +k_R + k_{NS} \end{bmatrix}_{N\times N} \quad \begin{matrix}[K_{n,b}]^T \\ [K_{n,c}]\end{matrix} = \begin{bmatrix} 0 & \cdots & -k_{NS} \\ 0 & \cdots & -k_R \end{bmatrix}_{2\times N} \quad [K_{n,d}] = \begin{bmatrix} +(k_{PS}+k_{NS}) & -k_{PS} \\ -k_{PS} & k_R + k_{PS} \end{bmatrix}_{2\times 2} \tag{A.3.2}$$

$$[C_{n,a}] = [0]_{N\times N} \quad [C_{n,b}]^T = [C_{n,c}] = [0]_{2\times N} \quad [C_{n,d}] = \begin{bmatrix} +c_{PS} & -c_{PS} \\ -c_{PS} & +c_{PS} \end{bmatrix}_{2\times 2} \tag{A.3.3}$$

**A.4 EKD**

The controlled system has (*N*+2) dynamic DoFs. The mass terms as the same as the Kdamper (A.3.1). The stiffness and damping submatrices Equations (3) are expressed as follows:

$$[K_{n,a}] = \begin{bmatrix} 0 & \cdots & 0 \\ \vdots & \ddots & \vdots \\ 0 & \cdots & +(k_R + k_{PS}) \end{bmatrix}_{N\times N} \quad \begin{matrix}[K_{n,b}]^T \\ [K_{n,c}]\end{matrix} = \begin{bmatrix} 0 & \cdots & -k_{PS} \\ 0 & \cdots & -k_R \end{bmatrix}_{2\times N} \quad [K_{n,d}] = \begin{bmatrix} +(k_{NS}+k_{PS}) & -k_{NS} \\ -k_{NS} & k_R + k_{NS} \end{bmatrix}_{2\times 2} \tag{A.4.1}$$

$$[C_{n,a}] = [0]_{N\times N} \quad [C_{n,b}]^T = [C_{n,c}] = [0]_{2\times N} \quad [C_{n,d}] = \begin{bmatrix} +c_{NS} & -c_{NS} \\ -c_{NS} & +c_{NS} \end{bmatrix}_{2\times 2} \tag{A.4.2}$$

**A.5 EKDI**

The only difference with the EKD is the addition of the inerter. The submatrices that differ from A4 are:

$$[M_{n,a}] = \begin{bmatrix} 0 & \cdots & 0 \\ \vdots & \ddots & \vdots \\ 0 & \cdots & -m_{top} + m_b \end{bmatrix}_{N\times N} \quad [M_{n,b}]^T = [M_{n,c}] = \{0\}_{2\times N} \quad [M_{n,d}] = \begin{bmatrix} +m_D & -m_b \\ -m_b & +(m_{top} + m_b) \end{bmatrix}_{2\times 2} \tag{A.5.1}$$